Engineering and Technology Journal e-ISSN: 2456-3358

Volume 09 Issue 09 September-2024, Page No.- 5065-5072

DOI: 10.47191/etj/v9i09.10, I.F. – 8.227

Early Hotspot Detection in Photovoltaic Modules using Deep Learning Methods

Belkıs Eristi

Electrical and Energy Department, Vocational School of Technical Sciences, Mersin University, Mersin, Turkey

https://orcid.org/0000-0003-1276-2347

ABSTRACT: Photovoltaic (PV) energy systems have been widely used in energy production especially in recent years due to their clean, reliable, environmentally friendly and resource continuity. The electrical energy to be obtained must be uninterrupted and of high quality. For this reason, faults that may cause production losses in PV power plants should be detected quickly and accurately. In this study, an approach that can automatically detect hotspot fault in solar PV modules is presented. In the proposed approach, firstly, Jet colormap based colored image transformation process is applied to gray scale infrared image data. Then, using three different deep learning models such as MobilNetV2, ResNet-18, InceptionV3, both original grey scale data and Jet colormap data are detected and evaluation metric values are obtained. The importance of this research lies in the potential of deep learning-based effective detection, especially in the early and rapid diagnosis of PV hotspot faults.

KEYWORDS: Photovoltaic module, Hotspot, Fault detection, deep learning models.

1. INTRODUCTION

In recent years, it has become widespread to include different sources in energy systems in order to meet the increasing demand for electrical energy with the development of technology. The use of fossil fuels in electrical energy production causes environmental pollution, serious health problems and disrupts the ecological balance. For this reason, renewable energy sources (RES) have begun to attract great attention all over the world in order to meet the demand for electrical energy [1-3]. Among the types of RES used, photovoltaic (PV) based energy systems attract attention due to their advantages such as being easily accessible, having high resource capacity, not being dependent on external resources, having low operating costs, being clean and reliable [2]. However, faults may occur in PV plants that affect the operating system and cause production losses. These may lead to reduced efficiency, reliability, continuity and some electrical risks [4]. Therefore, it is very important to detect faults that may occur in PV modules. Automatic fault detection is very important to ensure correct maintenance of PV power plant faults and to increase reliability and durability by ensuring continuity of energy production [5-6]. Many faults can occur in PV modules. One of the most common types of faults in PV modules is hotspot fault. PV hotspot is a fault that occurs especially as a result of partial shading, but can also occur with snail tracks and micro cracks, and can be defined as an unequal temperature increase between the temperatures of PV cells. In this case, the cell starts to emit heat energy instead of producing the electrical energy, which causes the temperature of the solar panels to increase. In order to extend the life of PV panels, hot spots need to be detected early. An automatic detection system is needed for fast and accurate hot spot fault detection in large PV plants [7]. In this paper, a system that can automatically detect hotspot faults in solar PV modules using three different deep learning models is proposed. In the proposed system, grey scale infrared image data is converted into colored image data by Jet colormap process to achieve an effective performance. Deep learning based detection process is performed for the original and colored PV module data. Evaluation metrics are also calculated for the obtained detection results. As a result, an effective approach for early detection of hotspot faults is achieved in this paper.

2. RELATED WORKS

There are many studies in the literature on the automatic detection of hotspot faults. In [8], a system based on hybrid features and a support vector machine (SVM) classifier is proposed. Hotspot detection and classification are performed using infrared thermographic images. Classification results are obtained in three classes as normal, faulty and hotspot. In order to verify the superiority of the proposed model and the hybrid feature dataset, different machine learning algorithms and datasets are compared. It can be seen that the hybrid features with SVM have a 92% test accuracy. In [9], four different machine learning methods are used for the detection of PV hotspots. Confusion matrix and receiver operating characteristics are also used to compare the performance of the four classifiers. In [10], a new multifunctional attention gate network is used for hot spot fault detection in PV panels. The proposed approach is validated with a real fault detection system, highlighting the effectiveness of the method. In [11],

a study on the classification of hotspot faults using deep learning methods is presented. In this study, data multiplexing is performed on the image data in the training dataset to increase the classification performance, and then six pre-trained deep learning models are compared on the same test dataset. It is seen that AlexNet have the best performance with an accuracy value of 98.65%. In [7], a new method for early hotspot detection is proposed using color image descriptors and a machine learning algorithm. In the presented method, thermographic images obtained from PV panels are divided into non-overlapping regions and color image descriptors are calculated for the regions. These color descriptors are then used to train different machine learning algorithms. The experimental results show that the k-Nearest Neighbor and Red-Green Scale-Invariant Feature Transform descriptors perform well with an accuracy rate of 98.7%. In [12], the hotspot effect in PV modules is analyzed for 2580 polycrystalline silicon PV modules distributed throughout the United Kingdom. The performance ratios of all PV modules are obtained. It is found that the average performance ratio is significantly reduced due to the presence of hotspots in PV modules. The performance ratios between normal and faulty PV modules are obtained with a minimum difference of -0.83% and a maximum difference of -15.47%. In [13], a machine learning based hotspot detection study is presented using infrared thermographic images of PV modules. Hotspots are classified using texture and histogram of gradient features of PV module images and Naive Bayes method. In the experimental results, it is seen that it has a success rate of approximately 94.1% for 375 sample sets. In [14], a fisheye lens model is developed for hotspot detection in PV modules. It is observed that the developed lens model can simultaneously monitor all rows of PV modules, each 100 m long. In [15], an active hotspot detection method is presented using ac parameter characterization to detect hotspots in PV cells. The PV cell impedance value change caused by the hotspot can be detected by monitoring a high-frequency measurement.

3. HOTSPOT DETECTION APPROACH

An intelligent decision-making mechanism can be developed by using deep learning approaches to improve energy production performance and early detection of hotspot faults in solar PV systems. Unlike traditional machine learning algorithms, deep learning-models offer effective solutions to the classification problems with their strong self-learning capabilities. In this paper, three different deep learning models are used to detect hotspot faults in solar PV modules. In order to achieve a more effective performance in this detection process, Jet colormap based colored image transformation process is first applied to gray scale infrared image data. Then, three different deep learning models are used to classify both the original grey scale data and the Jet colormap data. Finally, the detection results obtained are shown with evaluation metrics. Figure 1 shows the flow steps of the hotspot detection system presented in this paper.

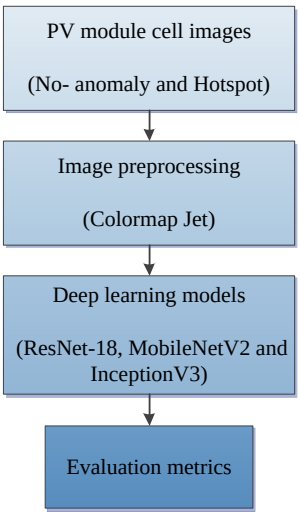

Figure 1. Framework of hotspot detection approach used in this study.

4. HOTSPOT DATASET

It is observed that hotspot fault events constitute 49% of all fault events in PV modules. The percentage of hotspot faults due to physical problems in the module is 25% and the percentage of hot spot faults due to diode damage is 24% [17]. PV cells experiencing hotspots have a higher temperature increase compared to normal cells around them. Using an infrared camera, color differences between hotspot cells and normal cells can be easily seen [14]. Hotspot faults can occur rapidly and continuously as they are affected by environmental conditions. Therefore, in order to ensure the reliability of the panels and extend their lifespan, it is very important to automatically detect faults in a timely and accurate manner. To evaluate the hotspot detection method presented in this paper, a publicly available and freely shared infrared solar modules dataset is used [16]. The infrared thermographic PV module images in the dataset consist of images belonging to a total of 12 classes, one of which is normal and the others are faulty, taken from real PV systems. Each of the data has a resolution of 24×40 pixels. These

images are collected by the Raptor Maps team using piloted aircraft and unmanned aerial systems equipped with mid-wave or long-wave infrared (3-13.5 µm) visible spectrum imaging systems [16]. Since hotspot fault detection is performed in this paper, 249 hotspot fault images, 246 multiple hotspot fault images and 500 no anomaly class images in the dataset are used. The number of data used and their descriptions are given in Table 1.

Table 1. The number of data used and their descriptions.

Class name	Number of images	Description
Hotspot	249	Hotspot on a thin film module.
Hotspot-Multi	246	Multiple hotspots on a thin film module.
No Anomaly	500	Nominal solar module.
Total	995	Total Number of Images.

In this paper, the data consisting of a total of 998 infrared images given in Table 1 is named as dataset-1. In addition, Jet colormap based colorization process is applied to these original data and dataset-2 is obtained. Figure 2 shows the images of 8 randomly selected image data in both dataset-1 and dataset-2.

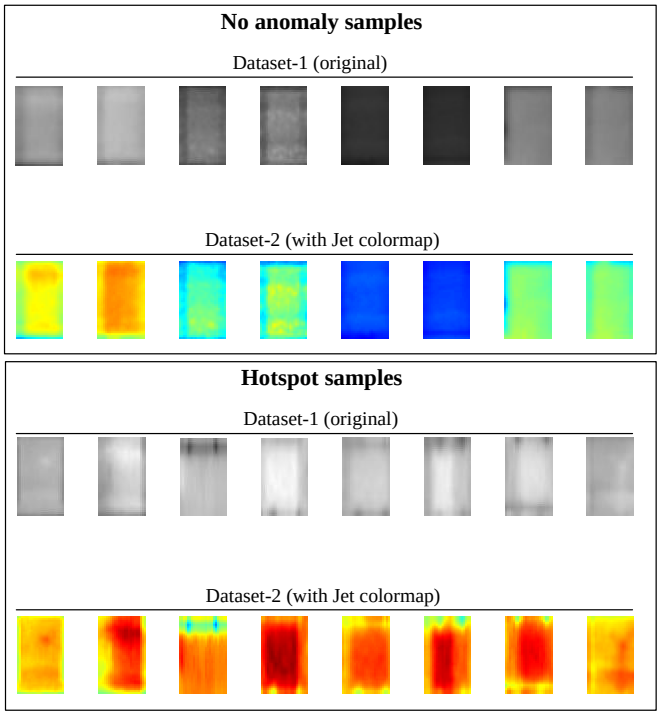

Figure 2. Infrared image data randomly selected from the datasets.

5. DEEP LEARNING MODELS

Deep learning models are widely used in image processing problems. In this paper, we used MobileNetV2, ResNet-18 and InceptionV3 models, which are pre-trained deep learning models. In this section, brief information about the general features of the models used is given.

The MobileNetV2 architecture is a preferred architecture for overfitting in recognition tasks when the dataset is relatively small for training, by using a smaller but expressive network. MobileNetV2 is also an architecture that optimizes low memory consumption and execution speed, making experimentation and parameter tuning much easier. There are two important concepts that define the MobileNetV2 architecture. These are depth-separable convolution and inverse residual. With these concepts, the network has a low-dimensional compressed representation feature that is extended to high dimensionality and filtered with a lightweight depth-based convolution [18]. The grouped convolutions in the network use 3x3 filter sizes, while the others use 1x1 filter sizes. The global average pool of MobileNetV2 is only one [11]. The structure of the MobileNetV2 architecture is shown in Figure 3

.

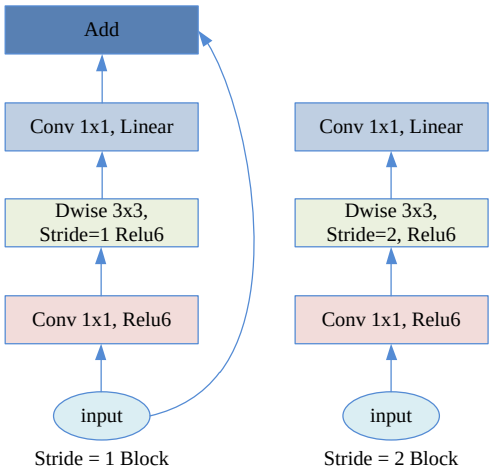

Figure 3. MobilNetV2 architecture structure [19].

ResNet architecture is an architecture that has won first prize in many areas in the ILSVRC and COCO2015 competitions it participated in [21]. ResNet architecture was developed by Kaiming He and his friends in 2015. ResNet-18 architecture is a deep learning model consisting of residual blocks. It is aimed to help the partial transfer of input information to the result and to make learning efficient by preventing the problem of gradient loss in model training thanks to shortcut connections called residuals [20]. The structure of ResNet-18 architecture is shown in Figure 4.

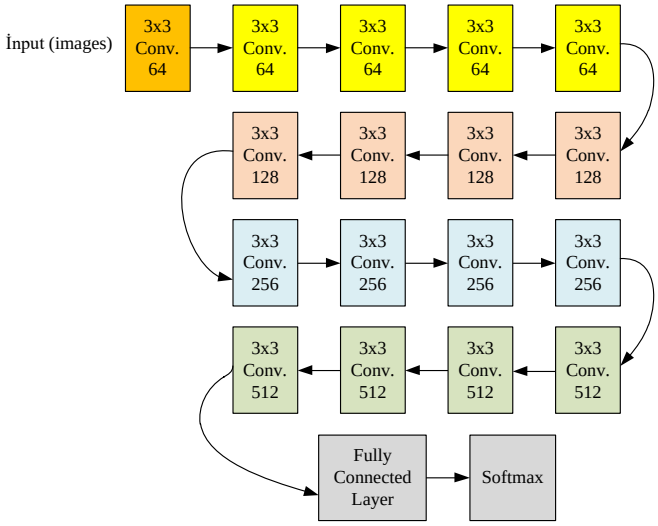

Figure 4. ResNet-18 Architecture structure [22].

The InceptionV3 architecture is deep and complex. It consists of a stack of interconnected Inception modules, each containing different types of convolution and pooling layers designed to extract different features from the input image. The use of factored convolutions, which allow the network to learn both local and global features of an image, is one of the key features of InceptionV3. This method increases the accuracy of the model by reducing the number of parameters in the network. Factored Convolution extracts features from the input image using 1×1, 3×3 and 5×5 convolutional filters. 1×1 convolutional filters reduce the size of the input image. 3×3 and 5×5 filters are used to extract more complex features from the input. Another important feature of InceptionV3 is that it uses a batch normalization technique. This technique helps to stabilize the training process while reducing the covariate drift, which is the change in the distribution of the network's inputs during training [23]. InceptionV3 layers consist of three standard convolution layers followed by a max pooling layer, two convolution layers and a max pooling layer. The next stage in the network includes the initial convolution, which simultaneously convolves the input using a different filter size for each convolution, further combining or stacking the results, and passing them through the network. The subsequent sections of the network are rested several times, starting from the beginning, where some sections repeat 10 or 20 times towards the end. The network applies the learning layer to randomly drop the weights to prevent overfitting. Also, the second last layer is fully connected [24]. The structure of the InceptionV3 architecture is shown in Figure 5

.

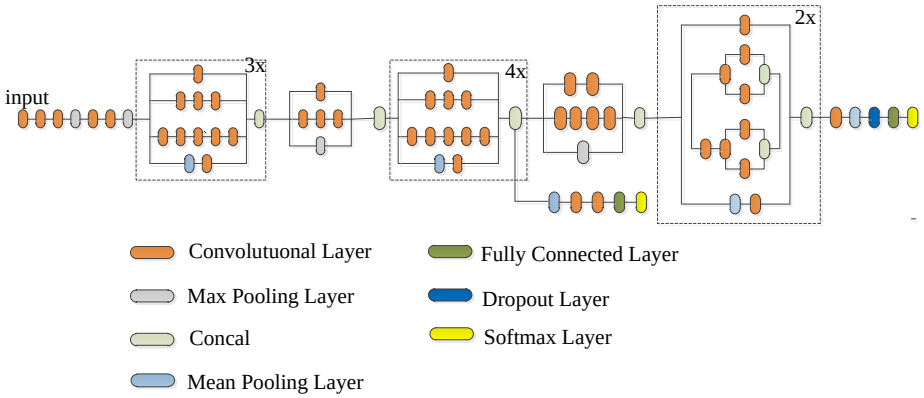

Figure 5. InceptionV3 Architecture structure.

6. EXPERIMENTAL STUDIES AND RESULTS

In this section, experimental studies on the detection of hotspots in PV modules are carried out. All experiments are performed on a computer with Intel (R) i7-12700KF 3.60 GHz CPU, NVIDIA GEFORCE RTX 4070 GPU and 32 GB RAM. In the experiments, 70% (697) of the datasets are allocated for training purposes, 15% (149) of the datasets are designated for validation, and 15% (149) of the datasets are reserved for testing. The detection approaches are created in Matlab R2022a environment. Table 2 shows the hyperparameters used for all deep learning algorithms.

Table 2. The Hyperparameters of all deep learning medels.

Optimizer	SGDM
Learning rate	1e3
MiniBatch size	32
Training epoch size	60

Data augmentation strategies have been applied to deep learning models for various purposes such as addressing the overfitting problem, expanding the dataset, and strengthening the model. Data augmentation is applied only to the training data, and the training set is augmented by 1) random reflection in the left-right direction, 2) ±45° rotation, and 3) translation by ±4 pixels. Figure 6 shows the results of a training process for dataset-2 data with the ResNet-18 model. As can be seen from the training process, the training has been completed in 1 minute 20 seconds with a very fast time.

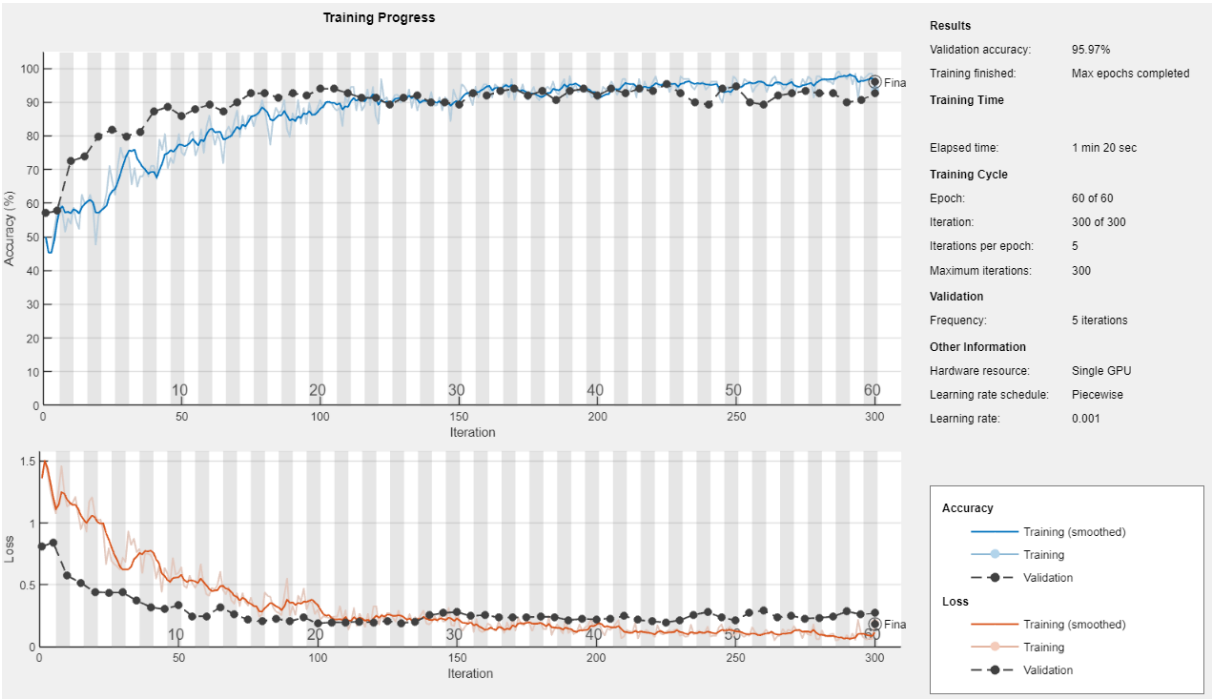

Figure 6. The result of a ResNet-18 training process for Dataset-2.

In order to statistically evaluate the detection results, some evaluation metrics such as accuracy (ACC), precision (PRE), sensitivity (SEN), specificity, SPE) and F1-score. These evaluation metrics are determined using four main results from the detection process. These are True Positive (TP), True Negative (TN), False Positive (FP) and False Negative (FN). These metrics are obtained using the following equations [25].

$$ACC=\frac{TP+TN}{TP+FN+TN+FP} \quad (1)$$

$$PRE=\frac{TP}{TP+FP} \quad (2)$$

$$SEN=\frac{TP}{TP+FN} \quad (3)$$

$$SPE=\frac{TN}{TN+FP} \quad (4)$$

$$F1\text{-}score=\frac{2\times TP}{2\times TP+FN+FP} \quad (5)$$

In order to evaluate the performance of the detection system presented in this paper, infrared solar module data are divided into two classes as no anomaly (c1) and hotspot faulty (c2) and fault detection results are obtained. The detection results obtained for dataset-1 and dataset-2 are given in Figure 7 as confusion matrices. As can be seen from the results obtained from the test set, the best results are obtained with the Jet colormap images (dataset-2). For this dataset, only five data are misclassified with ResNet-18 and MobilNetV2. The number of misclassified data for dataset-1 is nine.

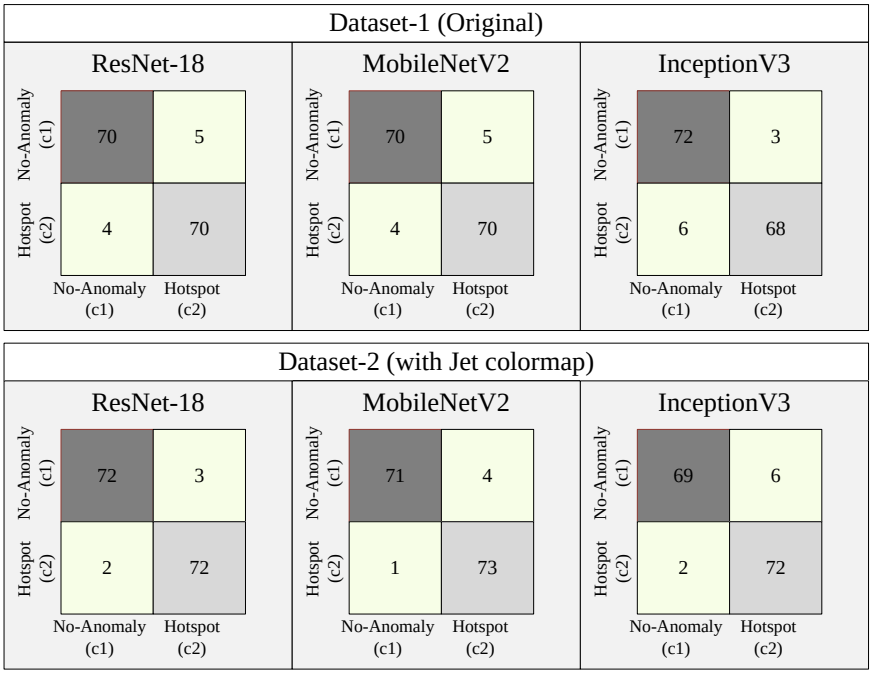

Figure 7. The confusion matrices of dataset-1 and dataset-2.

Evaluation metrics are calculated to determine the detection performance of the deep learning models for both datasets. The evaluation metric results are listed in Table 3. In this table, bold values indicate the best metric values. According to these bold values, the best detection results are obtained with ResNet-18 and MobileNetV2 deep learning models for dataset-2.

Table 3. Evaluation metric results of the proposed detection system.

Metrics	Dataset-1			Dataset-2		
	ResNet18	MobileNetV2	InceptionV3	ResNet-18	MobileNetV2	InceptionV3
ACC	0.9396	0.9396	0.9396	**0.9664**	**0.9664**	0.9463
PRE	0.9333	0.9333	0.9577	**0.9600**	0.9481	0.9231
SEN	0.9459	0.9459	0.9189	0.9730	**0.9865**	0.9730
SPE	0.9333	0.9333	0.9600	**0.9600**	0.9467	0.9200
F1-score	0.9396	0.9396	0.9379	0.9664	**0.9669**	0.9474

7. CONCLUSION

In this paper, an automatic hotspot fault detection of PV modules is performed using thermographic infrared PV module images. The data consisting of 998 original infrared images is named as dataset-1. Jet colormap based dataset-2 is obtained by transforming this original data (dataset-1). Then, using three different deep learning models (MobilNetV2, ResNet-18, InceptionV3), two classes of detection results, no anomaly (c1) and hotspot faulty (c2), are obtained. The confusion matrix of the detection results obtained for dataset-1 and dataset-2 are calculated. As can be seen from the results obtained from the test set, the best results are obtained with Jet colormap based data set-2. Besides, the best detection results are obtained with ResNet18 and MobileNetV2 deep learning models.

REFERENCES

1. Acikgoz, H. (2022). A novel approach based on integration of convolutional neural networks and deep feature selection for short-term solar radiation forecasting. *Applied Energy*, *305*, 117912.
2. Korkmaz, D. (2021). SolarNet: A hybrid reliable model based on convolutional neural network and variational mode decomposition for hourly photovoltaic power forecasting. *Applied Energy*, *300*, 117410.
3. Korkmaz, D., Acikgoz, H., & Yildiz, C. (2021). A novel short-term photovoltaic power forecasting approach based on deep convolutional neural network. *International Journal of Green Energy*, *18*(5), 525-539.
4. Korkmaz, D., & Acikgoz, H. (2022). An efficient fault classification method in solar photovoltaic modules using transfer learning and multi-scale convolutional neural network. *Engineering Applications of Artificial Intelligence*, *113*, 104959.
5. Haque, A., Bharath, K. V. S., Khan, M. A., Khan, I., & Jaffery, Z. A. (2019). Fault diagnosis of photovoltaic modules. *Energy Science & Engineering*, *7*(3), 622-644.
6. Espinosa, A. R., Bressan, M., & Giraldo, L. F. (2020). Failure signature classification in solar photovoltaic plants using RGB images and convolutional neural networks. *Renewable Energy*, *162*, 249-256.
7. Ali, M. U., Saleem, S., Masood, H., Kallu, K. D., Masud, M., Alvi, M. J., & Zafar, A. (2022). Early hotspot detection in photovoltaic modules using color image descriptors: An infrared thermography study. *International Journal of Energy Research*, *46*(2), 774-785.
8. Ali, M. U., Khan, H. F., Masud, M., Kallu, K. D., & Zafar, A. (2020). A machine learning framework to identify the hotspot in photovoltaic module using infrared thermography. Solar Energy, 208, 643-651.
9. Dhimish, M. (2021). Defining the best-fit machine learning classifier to early diagnose photovoltaic solar cells hot-spots. *Case Studies in Thermal Engineering*, *25*, 100980.
10. Su, B., Chen, H., Liu, K., & Liu, W. (2021). RCAG-Net: Residual channelwise attention gate network for hot spot defect detection of photovoltaic farms. *IEEE Transactions on Instrumentation and Measurement*, *70*, 1-14.
11. Açıkgöz, H., Korkmaz, D., & Dandıl, Ç. (2022). Classification of hotspots in photovoltaic modules with deep learning methods. Turkish Journal of Science and Technology, 17(2), 211-221.
12. Dhimish, M., Mather, P., & Holmes, V. (2018). Evaluating power loss and performance ratio of hot-spotted photovoltaic modules. *IEEE Transactions on Electron Devices*, *65*(12), 5419-5427.
13. Niazi, K. A. K., Akhtar, W., Khan, H. A., Yang, Y., & Athar, S. (2019). Hotspot diagnosis for solar photovoltaic modules using a Naive Bayes classifier. *Solar Energy*, *190*, 34-43.
14. Pramana, P. A. A., & Dalimi, R. (2020, December). Hotspot detection method in large capacity photovoltaic (PV) Farm. In *IOP Conference Series: Materials Science and Engineering* (Vol. 982, No. 1, p. 012019). IOP Publishing.
15. Kim, K. A., Seo, G. S., Cho, B. H., & Krein, P. T. (2015). Photovoltaic hot-spot detection for solar panel substrings using AC parameter characterization. *IEEE Transactions on Power Electronics*, *31*(2), 1121-1130.
16. Millendorf, M., Obropta, E., & Vadhavkar, N. (2020, April). Infrared solar module dataset for anomaly detection. In *Proc. Int. Conf. Learn. Represent*.

17. Deng, S., Zhang, Z., Ju, C., Dong, J., Xia, Z., Yan, X., ... & Xing, G. (2017). Research on hot spot risk for high-efficiency solar module. *Energy Procedia*, *130*, 77-86.
18. Buiu, C., Danaila, V., & Raduta, C. (2020). MobileNetV2 ensemble for cervical precancerous lesions classification, Processes, 8, 595.
19. Kulkarni, U., Gurlahosur, S. V., Babar, P., Muttagi, S. I., Soumya, N., Jadekar, P. A., & Meena, S. M. (2023, April). Facial Key points Detection using MobileNetV2 Architecture. In *2023 IEEE 8th International Conference for Convergence in Technology (I2CT)* (pp. 1-6). IEEE.
20. Çiftçi, S. Swin Tabanlı Dönüştürülmüş Görüntülerin Sınıflandırılması. *Harran Üniversitesi Mühendislik Dergisi*, *8*(2), 108-115.
21. Yu, X., & Wang, S. H. (2019). Abnormality diagnosis in mammograms by transfer learning based on ResNet18. *Fundamenta Informaticae*, *168*(2-4), 219-230.
22. Yüzgeç, E., & Talo, M. (2023). Alzheimer ve Parkinson Hastalıklarının Derin Öğrenme Teknikleri Kullanılarak Sınıflandırılması. *Fırat Üniversitesi Mühendislik Bilimleri Dergisi*, *35*(2), 473-482.
23. Minarno, A. E., Aripa, L., Azhar, Y., & Munarko, Y. (2023). Classification of malaria cell image using inception-v3 architecture. *JOIV: International Journal on Informatics Visualization*, *7*(2), 273-278.
24. Bhatia, Y., Bajpayee, A., Raghuvanshi, D., & Mittal, H. (2019, August). Image captioning using Google's inception-resnet-v2 and recurrent neural network. In *2019 Twelfth International Conference on Contemporary Computing (IC3)* (pp. 1-6). IEEE.
25. Hossin, M., Sulaiman, M. N. (2015). A review on evaluation metrics for data classification evaluations. *International journal of data mining & knowledge management process*, 5(2), 1.